

Connectivity of the Subthalamic Nucleus and Globus Pallidus Pars Interna to Regions Within the Speech Network: A Meta-Analytic Connectivity Study

Jordan L. Manes,¹ Amy L. Parkinson,² Charles R. Larson,³
Jeremy D. Greenlee,⁴ Simon B. Eickhoff,^{5,6} Daniel M. Corcos,⁷ and
Donald A. Robin^{2,8*}

¹Interdepartmental Neuroscience Program, Northwestern University, Evanston, Illinois

²The University of Texas Health Science Center, San Antonio, Texas

³Department of Communication Sciences and Disorders, Northwestern University, Evanston, Illinois

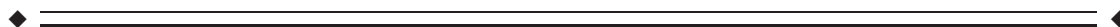
⁴Department of Neurosurgery, The University of Iowa, Iowa City, Iowa

⁵Department of Clinical Neuroscience and Medical Psychology, Heinrich-Heine University, Düsseldorf, Germany

⁶Institute for Neuroscience and Medicine (INM-1), Research Center Jülich, Germany

⁷Department of Kinesiology and Nutrition, The University of Illinois, Chicago, Illinois

⁸Honors College, The University of Texas at San Antonio, San Antonio, TX



Abstract: Cortico-basal ganglia connections are involved in a range of behaviors within motor, cognitive, and emotional domains; however, the whole-brain functional connections of individual nuclei are poorly understood in humans. The first aim of this study was to characterize and compare the connectivity of the subthalamic nucleus (STN) and globus pallidus pars interna (GPi) using meta-analytic connectivity modeling. Structure-based activation likelihood estimation meta-analyses were performed for STN and GPi seeds using archived functional imaging coordinates from the BrainMap database. Both regions coactivated with caudate, putamen, thalamus, STN, GPi, and GPe, SMA, IFG, and insula. Contrast analyses also revealed coactivation differences within SMA, IFG, insula, and premotor cortex. The second aim of this study was to examine the degree of overlap between the connectivity maps derived for STN and GPi and a functional activation map representing the speech network. To do this, we examined the intersection of coactivation maps and their respective contrasts (STN > GPi and GPi > STN) with a coordinate-based meta-analysis of speech function. In conjunction with the speech map, both STN and GPi coactivation maps revealed overlap in the anterior insula with GPi map additionally showing overlap in the supplementary motor area (SMA). Among cortical regions activated by speech tasks, STN was found to have stronger connectivity than GPi with regions involved in cognitive linguistic processes (pre-SMA, dorsal anterior insula, and inferior frontal gyrus), while GPi demonstrated stronger connectivity to regions involved in motor speech processes (middle insula, SMA, and premotor cortex). *Hum Brain Mapp* 00:000–000, 2013. © 2013 Wiley Periodicals, Inc.

Contract grant sponsor: National Institutes of Health; Contract grant number: DC006243; Contract grant sponsor: National Institutes of Mental Health; Contract grant number: MH074457.

*Correspondence to: Donald A. Robin, The University of Texas Health Science Center, San Antonio, Texas.
E-mail: robind@uthscsa.edu

Received for publication 30 April 2013; Revised 18 September 2013; Accepted 24 September 2013.

DOI 10.1002/hbm.22417

Published online 00 Month 2013 in Wiley Online Library (wileyonlinelibrary.com).

Key words: subthalamic nucleus; globus pallidus; motor speech; speech cognition; meta-analysis; connectivity

INTRODUCTION

The structures comprising the basal ganglia (BG) share in a diverse functional circuitry, enabling cognitive and affective information processing in addition to their involvement in motor control [Alexander and Crutcher, 1990; Middleton and Strick, 2000; Temel et al., 2005]. To perform these various processes, they rely on interactions with neighboring subcortical nuclei and regions within the neocortex. For instance, the execution of a limb movement involves the relay of inhibitory signals from the striatum to the globus pallidus pars interna (GPi), and subsequent disinhibition of thalamocortical connections to the motor cortices [Alexander, 1994].

Currently, cortico-basal ganglia (CBG) connections are thought to be parcellated into four major circuits—the motor circuit, limbic circuit, associative circuit, and oculomotor circuit [Alexander et al., 1986; Alexander and Crutcher, 1990]. Within this model, the BG limb motor circuit involves connections to the supplementary motor area (SMA), pre-motor cortex, and primary motor cortex (M1); while the oculomotor circuit projects to the frontal eye field and supplementary eye field. The BG limbic circuit is described with connections to the hippocampus, amygdala, and anterior cingulate. Finally, the cortical connections in the associative circuit include dorsolateral prefrontal cortex (DLPFC) and lateral orbitofrontal cortex.

As current models of CBG connections are largely derived from tracing and electrophysiology studies in animals, it is likely that they underestimate the extent of connectivity between BG structures and the human cortex—particularly in regions involved with higher order cognitive processes. Functional brain imaging now allows us to non-invasively map both structural and functional connections between structures in humans. In addition, it allows us to examine the functional connectivity of a single region of interest (ROI) to the rest of the brain. Using a structure-based quantitative meta-analysis, Postuma and Dagher [2006] examined the functional coactivation networks of regions within the striatum. The caudate nuclei were highly connected with regions in the frontal lobe, including dorsolateral prefrontal cortex (DLPFC), inferior frontal gyrus, and the insula. They also demonstrated coactivations with the anterior cingulate cortex (ACC), posterior parietal cortex (PPC), and thalamus. The putamen was coactive, not only with frontal, parietal, and cingulate regions but also with SMA, suggesting that the putamen is the striatal component involved in the CBG motor circuit. The study further suggests the presence of a dorso-ventral

striatal gradient by which the dorsal-most areas are associated with associative and motor networks and ventral areas are associated with affective circuits. By contrast, behaviorally filtered meta-analytic connectivity models (MACM) of the caudate generated by Robinson et al. [2012] illustrate the coactivation of the caudate with regions in cognitive, emotion, and action domains.

In this study, we focus on the connectivity of the STN and GPi. Unlike the striatum, whose functional connectivity has been described through meta-analysis [Postuma and Dagher, 2006; Robinson et al., 2012], task-based functional imaging [Simonyan et al., 2013], and resting state connectivity [Di Martino et al., 2008], STN and GPi have received less attention in the functional imaging literature. To our knowledge, only two studies have used functional imaging to investigate the whole-brain functional connectivity of STN in humans. Brunenberg et al. [2012] used diffusion tensor imaging (DTI) and resting state fMRI to parcellate the anatomical and functional connectivity of STN in healthy subjects. The study first examined whole brain resting state connectivity of STN and found significant correlations with activity in subcortical, frontal and temporal regions. In addition, further analyses demonstrated a functional parcellation of STN into a posterior lateral motor area and anterior medial limbic area. By contrast, others have parcellated STN into three functional regions subsuming motor, limbic, and associative areas of the STN [Lambert et al., 2012]. In comparing the resting state functional connectivity of STN in PD patients and healthy controls, Baudrexel et al. [2011] found that STN demonstrated greater connectivity to cortical motor regions in PD patients than in healthy controls. Between the two groups, no differences were found in the functional connectivity of STN to associative or limbic regions.

Meanwhile, the whole-brain functional connectivity of GPi has yet to be mapped. The GPi serves as a main output for the BG due to its inhibitory modulation of thalamic activity [Alexander and Crutcher, 1990]. In the motor circuit, it serves to inhibit thalamocortical projections to the motor and motor association cortices. Activity in the GPi is modulated by both direct and indirect pathways. Within the indirect pathway, the GPi receives excitatory inputs from STN, leading to inhibition of motor thalamus. Some closed-parallel models of CBG loops include the GPi within the motor circuit alone [e.g., Parent, 1990]. However, integrated open-loop models of CBG connections incorporate segments of GPi into motor, associative, and limbic circuits [Joel and Weiner, 1994]. Within the associative circuit, the GPi is part of an open associative pathway to cortical regions in the motor circuit, receiving input

from the striatum and projecting to the premotor cortex [Joel and Weiner, 1994]. Draganski et al. [2008] used diffusion weighted imaging to investigate the structural connectivity of basal ganglia structures to various regions within the cortex. When seeding the pallidum as a region of interest, the authors found the dorsal–medial portion to connect with limbic and associative cortical regions (orbitofrontal cortex, medial prefrontal cortex, orbitofrontal cortex, DLPFC, and anterior cingulate cortex) and the ventral–lateral region to connect with sensorimotor and oculomotor areas (premotor cortex, inferior parietal lobe, and precuneus). This is corroborated by the work of Parent and Hazarati [Hazarati and Parent, 1992; Parent and Hazarati, 1995] who describe the segregation of these three circuits within the GPi as including lateral motor region, medial associative region, and rostromedial limbic region.

Disruption of cortico-basal ganglia connections can lead to problems in a number of functional domains. In Parkinson’s disease, reduced dopaminergic input to the striatum leads to excessive inhibition of thalamic projections to motor cortex [Obeso et al., 2008]. Further, the presence of cognitive and affective symptoms in Parkinson’s disease suggests the additional disruption of the associative and limbic circuits [Dubois and Pillon, 1996; Farina et al., 1994; Jacobs et al., 1995; Thiel et al., 2003]. Likewise, the motor, cognitive, and emotional symptoms found in Huntington’s disease arise as a result of damage to the motor, associative, and limbic circuits [Joel, 2001]. The behavioral changes associated with CBG circuit disruption become even more complicated when the task requires the involvement of multiple functional domains.

One unique example of this is speech function, which calls upon both cognitive and motor processes. Though the relationship between speech and cortico-basal ganglia connections is unclear, a number of speech disruptions may be related to abnormal BG function [Alm, 2004; Simonyan and Ludlow, 2010]. As dopaminergic neurons degenerate in the substantia nigra (SN), most patients with PD present with some degree of hypokinetic dysarthria (characterized by reduced voice intensity, monotonicity, and mono-loudness) [Duffy, 2012]. It has also been hypothesized that aberrant cortico-basal ganglia connections play a role in stuttering, as fluency has been shown to improve with administration of dopamine antagonists [Alm, 2004; Wu et al., 1997; Civier et al., 2013]. Functional imaging has identified abnormal activation of BG structures in hypophonia [Liotti et al., 2003], stuttering [Fox et al., 1996; Watkins et al., 2008], and spasmodic dysphonia [Ali et al., 2006; Haslinger et al., 2005; Simonyan and Ludlow, 2010].

Recently, Simonyan et al. [2013] examined the influence of speech-induced dopamine release on both the functional and structural striatal-speech network. After establishing speech-induced dopaminergic activity in the anterior putamen, the authors seeded the region in a functional connectivity analysis of overt speech production. The anterior putamen was found to have positive functional connections

with right IFG, left STG, cerebellum, and pons. It was also found to be negatively correlated with activity in the left laryngeal sensorimotor cortex, premotor cortex, SMA, SN/STN, right sensorimotor cortex (SMC), precuneus, and cerebellum. The authors go on to note that the regions within this network represent a variety of speech processes including motor output and phonological processing.

By contrast, the connectivity of STN and GPi to regions within the functional speech network has yet to be studied. Evidence from clinical trials in Parkinson’s disease have shown that the use of STN or GPi as surgical targets can lead to worsening of speech [Klostermann et al., 2008; Theodoros et al., 2000]. In earlier studies, lesions of the globus pallidus were used to attenuate the overactive inhibitory signals coming from the GPi. While this approach proved useful for improving general motor function, it was frequently accompanied by speech deterioration [Murdoch, 2010; Scott et al., 1998; Tasker et al., 1997; Theodoros et al., 2000]. Similarly, deep brain stimulation of the STN results in improved motor outcomes, but is frequently accompanied by worsening of speech function [Dromey and Bjarnson, 2011; Klostermann et al., 2008; Murdoch, 2010] and verbal fluency [Dietz et al., 2013; Parsons et al., 2006]. Although there is not yet a clear role for either of these structures in speech production, disrupted function of these regions can lead to overarching effects on motor and associative thalamocortical loops, both of which are required for normal speech processing.

The first aim of this study was to characterize and compare the connectivity of STN and GPi using meta-analytic connectivity modeling (MACM). The MACM technique uses pooled neuroimaging coordinates and metadata to (a) examine whole-brain coactivations with a pre-defined seed region across multiple experiments (unconstrained by task) and (b) describe the behavioral characteristics of the tasks contributing to those activations [Laird et al., 2009; Robinson et al., 2010]. Unlike traditional functional connectivity analyses, which are limited to either resting-state or task-specific data, MACM allows us to perform a quantitative coordinate-based meta-analysis that is constrained by coactivation with a defined region of interest (ROI) while being unconstrained by any specific task. The derivation of seed-to-whole brain connectivity models from pooled neuroimaging coordinates has been used to describe functional connectivity of the amygdala [Robinson et al., 2010], default mode network [Laird et al., 2009], cingulate cortex [Torta and Cauda, 2011], insular cortex [Cauda et al., 2012], and caudate [Robinson et al., 2012]. In addition, connectivity models derived from the BrainMap database have demonstrated high correspondence to both resting state [Laird et al., 2011; Smith et al., 2009] and diffusion tensor imaging data [Eickhoff et al., 2011; Robinson et al., 2012]. Here, we generated meta-analytic connectivity models from bilateral STN and GPi seeds to examine task-related whole-brain connectivity for each region independently.

The second aim of this study was to examine the degree of overlap between the connectivity maps derived for STN

and GPi and a functional activation map representing the speech network. To achieve this, we performed a task-based activation likelihood estimation (ALE) meta-analysis of speech behaviors encompassing a broad range of tasks. We were then able to perform conjunction analyses with STN and GPi connectivity maps to determine (a) the areas involved in speech processing which are functionally connected to our seed regions, and (b) the areas involved in speech processing which preferentially coactivate with one seed or the other.

We anticipated that the functional connectivity of STN and GPi would, to some degree, reflect the anatomical connectivity observed in animal models [e.g., Temel et al., 2005] and resting state connectivity models in humans [Brunenberg et al., 2012]. Because of the coupling of activity of STN and GPi via the indirect pathway, overlap between the functional connectivity networks of these two regions was expected. With respect to subcortical nuclei, we anticipated the coactivation of both STN and GPi with the thalamus and their other basal ganglia structures (striatum, pallidum, and substantia nigra). Because of their roles in motor, associative, and limbic circuits, we also hypothesized that STN and GPi seeds would coactivate with regions in the motor network (M1, SMA), frontal areas involved in cognitive processing, and regions of the limbic system (ACC). Coactivation differences between STN and GPi were also anticipated, as both regions receive input via other pathways (e.g., the direct pathway for GPi, and the “hyperdirect” pathway connecting STN to SMA). In relation to our interest in speech we expected to find a significant intersection of both STN and GPi connectivity maps with a functional meta-analytic map of speech function. Given that M1, premotor cortex, and SMA are all regions involved in speech production, we expected that the convergence of MACMs with the functional speech map would reveal overlap in these regions. In addition, we sought to determine whether the convergence of these maps was restricted to regions in the motor network or if they subsumed additional cortical areas. We predicted that the conjunction of the speech map with STN and GPi MACMs would indeed reveal significant functional overlap in areas outside the motor network.

MATERIALS AND METHODS

Data

Functional connectivity analyses were performed using the BrainMap database (www.brainmap.org), which archives published whole-brain neuroimaging data, including activation coordinates (foci) and associated metadata. The latter also classifies each experiment based on the behavioral domain (BD) and paradigm class (PC) that drove the reported activations. At the time of the analysis, the BrainMap database contained 2,238 published functional neuroimaging papers containing 10,646 experiments from

42,660 subjects and reporting a total of 85,007 activation foci (coordinate locations). This provided us with a rich data set to look for coactivations with STN and GPi across the entire brain while exploring the heterogeneity of tasks and behaviors driving those activations. It also allowed us to derive a meta-analytic map representative of the “speech network” by pooling activation coordinates elicited from a broad variety of speech tasks.

ROI Definition and Search Criteria

ROIs for bilateral STN and GPi were generated in MNI space (<http://ric.uthscsa.edu/mango/>) using the AAL Atlas definitions provided in MANGO (Fig. 1a). The ROI masks generated for left and right STN were 138 mm³ and 116 mm³, respectively (left centroid at -10, -9, -1; right centroid at 11, -10, -1). The ROI masks generated for left and right GPi were 548 mm³ and 590 mm³, respectively (left centroid at -12, 2, 2; right centroid at 11, 2, 2). To obtain data for the meta-analytic connectivity models, the BrainMap database was searched for functional imaging experiments reporting activation coordinates within each ROI. All experiments included in the final connectivity analyses met the following criteria: (a) subjects were classified as normal/healthy controls, (b) experimental context was normal mapping, (c) all experiments were group studies, and (d) significant activations were reported within the specified ROI (either STN or GPi). To compare these connectivity models to a functional speech network, we then conducted an additional search for experiments reporting activation coordinates during speech tasks. As the range of speech processes affected by the BG is still unclear, we broadly defined speech using the behavioral domain definitions provided in BrainMap. Studies included in the task-based speech meta-analysis met the following criteria: (a) subjects were classified as normal/healthy controls, (b) experimental context was normal mapping, (c) all experiments were group studies, and (d) the behavioral domain of the experiment was classified as either “Action.Execution.Speech” or “Cognition.Language.Speech” within the BrainMap taxonomy. Experiments examining disease effects, age effects, or task-related deactivations were excluded from all analyses.

Activation Likelihood Estimation

Foci indicating coordinates of activation were accumulated from each experiment that met the search criteria above. Statistical images were then created using the activation likelihood estimation method [ALE; Eickhoff et al., 2009, 2012; Turkeltaub et al., 2002, 2012]. The ALE approach tests the convergence of activation probability distributions across experiments against a null hypothesis of independently distributed foci across experiments. For each experiment, modeled activation (MA) maps were generated by converting foci into probability distributions

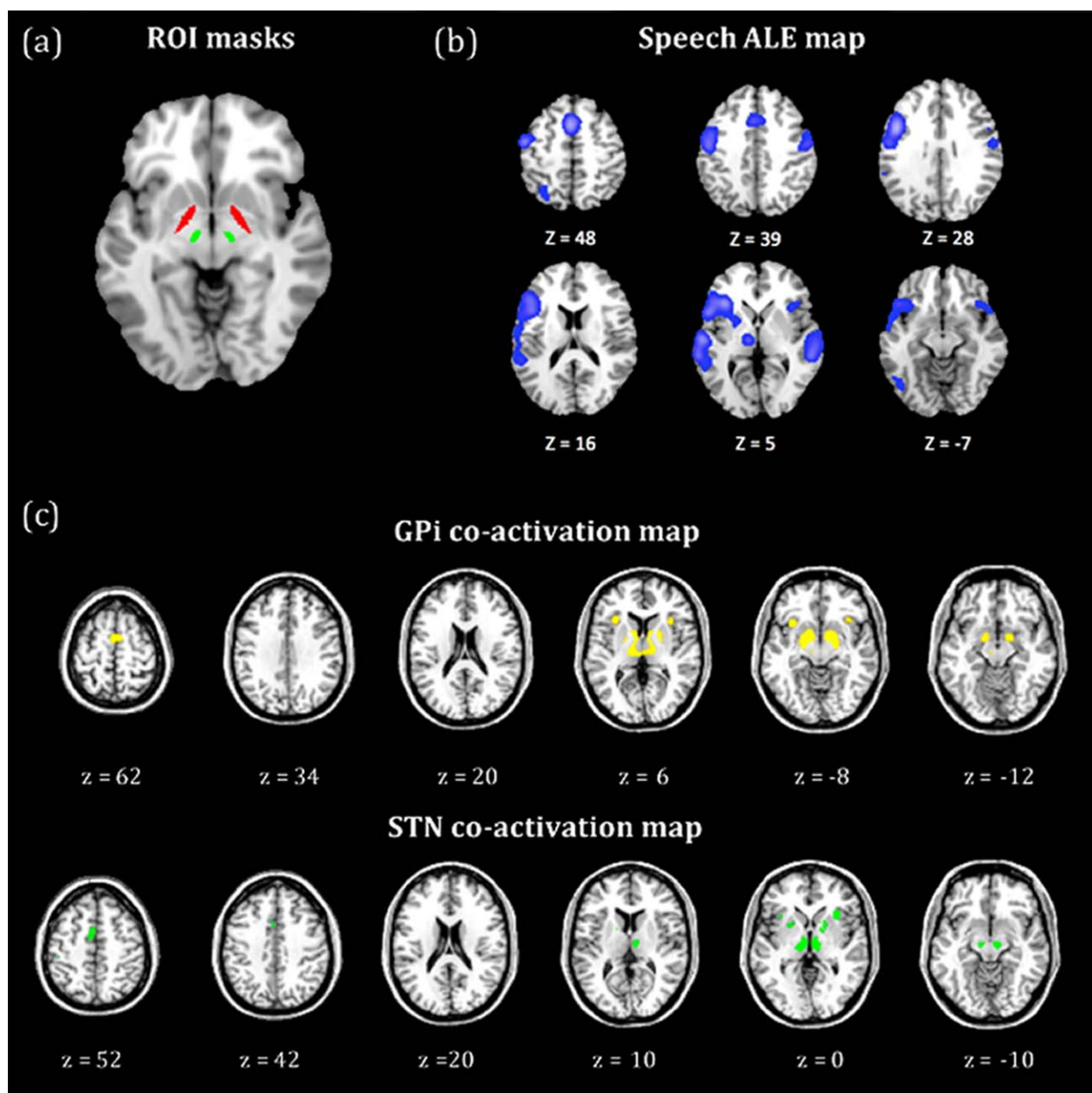


Figure 1.

(a) Region of interest masks for bilateral STN (green) and GPi (red). (b) ALE map of areas active during the performance of speech tasks; blue areas indicate significant convergence of foci across speech imaging experiments ($P < 0.05$, FWE corrected). (c) Meta-analytic connectivity models of GPi (above) and STN (below); colored regions indicate areas of significant coactivation with each region of interest ($P < 0.05$, FWE corrected).

centered at the reported activation coordinates. Probability distributions consisted of full width half maximum (FWHM) Gaussian distributions modified to account for spatial uncertainty [Eickhoff et al., 2009]. ALE scores were then generated to reflect the union of activation probabilities across experiments for each voxel in the brain. To

prevent multiple foci in a single experiment from influencing the ALE value of any one voxel, the probability distribution of the focus nearest the voxel in question was taken for each experiment [Turkeltaub et al., 2012]. For comparison, a null distribution of ALE values was derived from the integration of histograms. The experimental ALE

values were then tested against the null ALE values, yielding a P value for each ALE score. These P values were then converted into z -scores for statistical analysis. ALE images generated for the task-constrained meta-analysis of speech production were subjected to a threshold of $P < 0.05$, family-wise error (FWE) corrected. For each meta-analytic connectivity model, significant coactivations were also thresholded at $P < 0.05$, FWE corrected.

Differences in coactivation between STN and GPi MACMs were examined by first computing the voxel-wise difference between ALE maps [see Eickhoff et al., 2011]. Experiments from both STN and GPi analyses were then pooled together and randomly divided into two groups. The size of these groups was determined by the number of experiments contributing to each individual analysis (e.g., 51 experiments for STN and 144 experiments for GPi). This process was repeated 10,000 times to yield a null-distribution for the differences of ALE scores between STN and GPi seeds. The observed differences between STN and GPi ALE scores were then compared to this null-distribution. This yielded a P value for the ALE score difference at each voxel. The resultant P values were thresholded at a posterior probability of $P > 0.95$ and implicitly masked by the main effects of each individual MACM analysis [Eickhoff et al., 2011]. This method was further used to contrast the left and right hemisphere seeds within each ROI (e.g., left vs. right STN) to examine the effects of lateralization on coactivation patterns.

Minimum statistic conjunction analyses were then performed by computing the intersection of thresholded ALE maps [Eickhoff et al., 2011]. We first examined the conjunctions of STN and GPi ALE maps to look for common coactivations between each ROI. We then computed the intersections of STN and GPi ALE maps with the ALE maps derived from the speech meta-analysis ($STN \cap \text{Speech}$ and $GPi \cap \text{Speech}$). This allowed us to view the convergence of each ROI's functional connectivity with regions associated with speech function. Finally, to examine the degree to which converging regions preferentially coactivated with STN or GPi, we evaluated the conjunction of the speech ALE map with $STN > GPi$ and $GPi > STN$ contrast images ($\text{Speech} \cap STN > GPi$ and $\text{Speech} \cap GPi > STN$).

Functional Characterization Analysis

Activation coordinates archived in the BrainMap database are accompanied by meta-data describing the behaviors and paradigms associated with their respective experimental contrasts. Within the BrainMap taxonomy, behavioral domains (BD) describe five main categories of mental processes (action, cognition, perception, emotion, and interoception) along with their related subcategories (a complete list of behavioral domains can be found at <http://brainmap.org/scribe>). In addition, the specific task used for a given study is described by experiment's para-

digm class (PC). Functional profiles of STN and GPi were generated using a forward inference approach that identifies BD or PC categories for which the likelihood of observing activation in a given region (e.g., STN) is greater than overall probability of observing activation in that region in the BrainMap database. To do this, we first identified experiments reporting activation coordinates in each ROI. A baseline probability of activation for each ROI, or "base rate," was established by calculating the probability that a random activation within the BrainMap database would be found in that region. For each BD and PC label, we then calculated the conditional probability of observing activation in the ROI given the known functional characterization of foci within that region [$P(\text{Activation} | \text{Domain})$ and $P(\text{Activation} | \text{Paradigm})$]. The likelihood of activation in a region (STN or GPi) given a specific BD or PC was then compared to the base rate likelihood of activation using a binomial test ($P < 0.01$, uncorrected).

RESULTS

Literature Search

We searched the BrainMap database for experiments reporting activation coordinates in response to speech tasks. This search produced 906 experiments reporting 8,728 activation coordinates (209 papers, 3,215 subjects). In collecting data for the MACM of STN, our BrainMap search yielded 51 experiments reporting 961 activation coordinates in bilateral STN (data from 45 papers, 691 subjects). For the MACM of GPi, our search revealed 144 experiments reporting 2,415 activation coordinates in bilateral GPi (data from 119 papers, 1,894 subjects). Details of our search results are summarized in Table I.

Meta-Analysis of Speech Production

ALE maps were generated from speech-related activation coordinates to depict areas of significant activation ($P < 0.05$, FWE corrected). A list of these results can be found in Table II. Significant ALE values were reported in the left IFG/precentral gyrus, SMA, insula, postcentral gyrus, STG, superior parietal lobule, middle and inferior occipital gyri, thalamus, and cerebellum (Fig. 1b).

Meta-Analytic Connectivity Models

Connectivity models were generated from the published activation coordinates to examine task-induced coactivations of STN and GPi with all other regions in the brain (Fig. 1c, Table III). The MACM of our bilateral STN ROI resulted in significant bilateral coactivations with thalamus, putamen, and anterior insula, ($P < 0.05$, FWE corrected). Significant unilateral coactivations were observed in left SMA, left GPi, and left caudate ($P < 0.05$, FWE corrected). In the MACM of bilateral GPi, peak coactivations

TABLE I. Number of papers, experiments, subjects, and foci resulting from BrainMap searches of speech function and ROI coactivation in healthy controls

	Papers	Experiments	Subjects	Foci
Speech	209	906	3,215	8,728
Bilateral STN	45	51	691	961
Left STN	28	32	423	610
Right STN	22	23	338	413
Bilateral GPi	119	144	1,894	2,415
Left GPi	69	76	1,114	1,170
Right GPi	70	82	1,089	1,617

were found in right GPe, bilateral insula, right SMA, left substantia nigra, and left premotor cortex ($P < 0.05$, FWE corrected).

Contrast and conjunction analyses were conducted to assess the differences and commonalities of STN and GPi connectivity maps (Table IV; Fig. 2). Our conjunction analysis showed STN and GPi to share common coactivations with right lentiform nucleus, right thalamus, right insula, SMA, and left IFG. When contrasted, the GPi seed region demonstrated greater coactivation with bilateral GPe, left premotor cortex, left ventral IFG, left precentral gyrus, and right dorsal SMA than did STN ($P > 0.95$). In the STN > GPi contrast, STN resulted in greater connectivity to right subthalamic nucleus, bilateral putamen, bilateral insula, right middle cingulate cortex (MCC), bilateral inferior parietal lobe (IPL), left dorsal IFG, left SMA, right premotor cortex, left amygdala, right precentral gyrus, and left postcentral gyrus ($P > 0.95$).

Left Versus Right Hemisphere ROIs

In addition to examining the connectivity of our bilateral ROIs, we performed individual MACM analyses on the

left and right hemisphere nuclei (Table V). The results of these analyses revealed that left STN coactivated with left and right thalamus, SMA, right insula, right putamen, left inferior parietal lobule, right IFG, and left GPi ($P < 0.05$, FWE corrected). However, a lesser degree of connectivity was found in the MACM of right STN, in which coactivations were only seen in left and right thalamus ($P < 0.05$, FWE corrected). Our MACM of left GPi revealed significant coactivations with left GPi, right GPe, SMA, left and right insula, right thalamus, left precentral gyrus, and left STN ($P < 0.05$, FWE corrected). Right GPi demonstrated similar patterns of connectivity with coactivations in left and right GPi, left and right insula, SMA, right thalamus, and left GPe ($P < 0.05$, FWE corrected).

Significant differences in connectivity emerged from the comparison of left versus right STN ($P > 0.95$) and left versus right GPi ($P > 0.95$; Fig. 3). Contrasts of Left > Right STN demonstrated greater connectivity of left STN to left thalamus, left GPi, left IFG, bilateral post-central gyrus, right IPL, and left middle cingulate than right STN. The contrast of Right > Left STN revealed significantly stronger connectivity of right STN to the right brainstem, right precentral gyrus, left dorsal SMA, and left IPL compared to left STN. Left GPi showed significantly greater coactivations with left globus pallidus, left premotor cortex, left SMA, left thalamus, right putamen, and bilateral IFG compared to right GPi. Right GPi demonstrated greater connectivity to right globus pallidus, left insula, right IPL, right IFG, right SMA, right brainstem, right middle cingulate, left thalamus, left putamen, left subcallosal gyrus, and right rolandic operculum.

Conjunction of STN and GPi MACMs to Speech Meta-Analysis

To characterize the relationship of STN and GPi connections to the functional speech network, we performed

TABLE II. Regions demonstrating significant convergence across speech experiments

Location	MNI coordinates			z-Score	Size (voxels)
	x	y	z		
Left inferior frontal gyrus/pre-central gyrus	-44	12	26	3.55	6,975
Left supplementary motor area	0	8	56	3.23	1,500
Right superior temporal gyrus	56	-34	6	2.77	1,117
Right post-central gyrus	52	-8	36	2.62	718
Left inferior occipital gyrus	-44	-62	-14	2.65	549
Right insula	36	20	0	2.84	460
Right declive	22	-60	-22	2.78	337
Left thalamus	-10	-16	4	2.75	272
Left superior parietal lobule	-28	-62	46	2.16	156
Left declive	-14	-62	-18	2.54	79
Left middle occipital gyrus	-28	-94	-2	2.25	40

Peak MNI coordinates, z-scores, and volumes are reported for clusters exceeding a threshold of $P < 0.05$, FWE corrected.

TABLE III. Regions demonstrating significant coactivation with STN and GPi

Location	MNI coordinates			z-Score	Size (voxels)
	<i>x</i>	<i>y</i>	<i>z</i>		
GPi					
Right globus pallidus	16	-2	-2	8.55	1,756
Left insula	-32	20	-4	8.29	260
Right SMA	0	2	56	7.84	258
Right insula	36	20	0	8.08	223
Left substantia nigra	-8	-16	-8	5.41	9
Left premotor cortex	-34	-10	60	5.24	6
STN					
Right thalamus	10	-14	-2	8.39	317
Left thalamus	-10	-14	-2	8.40	256
Left SMA	-2	4	50	6.36	151
Right insula	34	20	2	7.09	98
Right putamen	18	10	-2	7.29	86
Left putamen	-24	8	0	5.69	24
Left caudate	-12	6	6	5.82	11
Left insula	-34	20	0	5.26	9
Left globus pallidus	-16	-6	-4	6.38	6

Peak MNI coordinates, z-scores, and volumes are reported for clusters exceeding a threshold of $P < 0.05$, FWE corrected.

conjunction analyses of bilateral STN and GPi MACMs with the speech network derived from our meta-analysis (Table VI, Fig. 4a). Significant intersection of $STN \cap Speech$ was found in the left insula, left ventral lateral nucleus (VLN) of the thalamus, left putamen, left GPi, and the right red nucleus. Further, the MACM of GPi intersected the speech network ($GPi \cap Speech$) in the left insula, right SMA, left putamen, left VLN, and right MDN.

We additionally used conjunction analyses to compare the contrasts of STN and GPi to the speech network (Table VI, Fig. 4b). This allowed us to examine which regions associated with speech were preferentially co-active with either STN or GPi. The conjunction of $Speech \cap STN > GPi$ resulted in significant activations among the left putamen, left dorsal anterior insula, left pre-SMA, and left inferior frontal gyrus (BA 44). In addition, the conjunction of $Speech \cap GPi > STN$ resulted in significant activation of left ventral anterior insula, left middle insula, left SMA, and left premotor cortex.

Functional Characterization of STN and GPi

After examining the coactivations of STN and GPi ROIs in the BrainMap database, we probed the meta-data of the same set of experiments to determine which tasks and behavioral domains made significant contributions to activity within our ROIs ($P < 0.01$, uncorrected; Fig. 5). Behavioral domains significantly associated with GPi activation were cognition, emotion, sadness, sexual interoception, and action inhibition. The experimental paradigms demonstrating significant association with GPi activation included reward tasks, finger tapping, flexion/extension,

episodic recall, and film viewing. STN activation was significantly associated with pain perception and action execution behavioral domains. Experimental paradigms significantly associated with STN activation were finger tapping, pain monitoring/discrimination, and reward tasks. The only common paradigm resulting from the conjunction analysis of STN and GPi was the reward task paradigm. Contrast analyses revealed that GPi maintained a significantly greater association with sexual interoception and emotion behavioral domains than STN. Paradigms with stronger relationships to GPi activation included face monitoring/discrimination tasks and passive viewing tasks. STN activation demonstrated significantly stronger associations with pain perception and pain monitoring/discrimination tasks than GPi.

DISCUSSION

Meta-Analytic Connectivity of STN and GPi

The first aim of our study was to characterize and compare the coactivations of STN and GPi. By performing a conjunction analysis of $STN \cap GPi$ we found that each of our ROIs shared coactivations with all nodes of the subcortical basal ganglia circuitry (caudate, putamen, thalamus, STN, GPi, and GPe). Within the cortex, convergence of STN and GPi MACMs occurred in SMA, insula, and IFG, which are involved in motor preparation/initiation [Eccles, 1982; Hanakawa et al., 2008], and imagination of motor tasks [Gerardin et al., 2000; Grafton et al., 1996].

Importantly, STN and GPi also displayed significant differences in coactivation with cortical and subcortical regions. While common to both STN and GPi MACMs,

TABLE IV. Results from conjunction ($\text{GPi} \cap \text{STN}$) and contrast ($\text{GPi} > \text{STN}$, $\text{STN} > \text{GPi}$) analyses of STN and GPi ALE maps

Location	MNI coordinates			z-Score	Size (voxels)
	<i>x</i>	<i>y</i>	<i>z</i>		
$\text{GPi} \cap \text{STN}$					
Right lentiform nucleus	18	8	-2	7.12	374
Right thalamus	14	-14	0	8.30	1,837
Right insula	34	20	2	7.09	441
Left inferior frontal gyrus	-52	8	20	4.01	63
Left supplementary motor area	-2	2	52	6.02	645
$\text{GPi} > \text{STN}$					
Right globus pallidus	12	0	-8	8.13	231
Left globus pallidus	-14	-2	-6	8.13	366
Left inferior frontal gyrus	-50	18	-2	1.87	7
Left premotor cortex	-36	-8	48	2.37	65
Left precentral gyrus	-46	8	48	1.85	10
Right supplementary motor area	12	-4	62	2.07	19
$\text{STN} > \text{GPi}$					
Right subthalamic nucleus	10	-16	-8	8.13	783
Left amygdale	-22	-4	-16	2.71	24
Right putamen	20	12	-2	3.26	96
Right insula	30	22	2	2.26	108
Left putamen	-22	10	2	3.00	137
Left insula	-40	4	4	2.05	41
Left inferior frontal gyrus	-54	10	26	2.59	52
Right middle cingulate gyrus	8	22	32	2.47	53
Left supplementary motor area	-6	10	52	3.67	603
Left inferior parietal lobule	-30	-50	40	3.38	118
Right precentral gyrus	40	2	44	3.54	176
Right inferior parietal lobule	36	-46	50	3.94	156
Left post-central gyrus	-46	-30	48	3.45	119

Peak MNI coordinates, z-scores, and volumes are reported for clusters demonstrating common activation between STN and GPi ALE maps ($\text{GPi} \cap \text{STN}$; $P < 0.05$) as well as clusters demonstrating significant differences between STN and GPi ALE maps ($\text{GPi} > \text{STN}$, $\text{STN} > \text{GPi}$; $P > 0.95$).

connectivity to SMA was significantly greater with the STN seed. Along with thalamocortical connections to SMA (modulated by the GPi), a direct fiber pathway has been proposed in which SMA and STN are connected by independent fiber pathways that do not pass through the thalamus, globus pallidus, or striatum [Brunenberg et al., 2012]. The presence of an additional “hyperdirect” pathway could explain the greater coactivation of SMA with STN observed in this study. Previous experiments have indeed shown decreased rCBF in SMA as a result of STN stimulation [Hershey et al., 2003; Karimi et al., 2008; Narayana et al., 2009]. However, it is interesting to note that while STN stimulation reduces rCBF in SMA at rest and during speech execution, it increases rCBF in SMA during the performance of other motor tasks [Ballanger et al., 2009].

Left premotor cortex was more strongly connected with GPi than STN. The connectivity of GPi to premotor cortex has been illustrated in both segregated and integrated models of thalamocortical circuits [Alexander and Crutcher, 1990; Joel and Weiner, 1994]. While the

pallidal-thalamic-premotor pathway is used to describe the motor circuitry of the basal ganglia alone, it has also been proposed to be an open pathway integrating the motor and associative BG circuits [Joel and Weiner, 1994]. Given that the coactivation of premotor cortex was stronger for GPi than STN, it is likely that this connection is modulated via striatal input in the direct pathway as opposed to subthalamic input in the indirect pathway.

Differences in coactivation of STN and GPi were also observed in frontal regions of the cortex. Within the IFG, STN demonstrated significantly stronger coactivations with BA 44 while GPi was more strongly connected with a more ventral portion of IFG. Another “hyperdirect” anatomical connection between IFG to STN has been observed using diffusion weighted tractography, and it has been proposed that the connections between STN, IFG, and pre-SMA comprise a network that facilitates response inhibition [Aron et al., 2007]. By contrast, the connectivity of IFG to GPi has primarily been described through indirect connections via STN or the striatum [e.g., Jahfari et al., 2011].

TABLE V. Coactivation differences between left and right hemisphere regions of interest

Location	MNI coordinates			z-Score	Size (voxels)
	<i>x</i>	<i>y</i>	<i>z</i>		
Left > Right STN					
Left middle cingulate gyrus	-8	4	42	3.00	214
Right post-central gyrus	54	-22	38	3.38	143
Left post-central gyrus	-42	-26	48	2.06	133
Left thalamus (VLN)	-8	-10	-6	8.13	129
Left inferior frontal gyrus	-46	10	22	2.35	89
Right inferior parietal lobule	44	40	52	2.08	29
Left GPi	-16	-6	-4	6.75	16
Right > Left STN					
Right brainstem	10	-16	-8	8.13	263
Right pre-central gyrus	36	-4	48	3.11	127
Left inferior parietal lobule	-26	-48	42	2.33	54
Left supplementary motor area	-10	0	58	2.14	15
Left > Right GPi					
Left globus pallidus	-16	-6	-6	8.13	424
Left premotor cortex	-38	-6	40	2.58	65
Right inferior frontal gyrus	52	4	18	2.30	27
Left supplementary motor area	-12	8	62	1.81	19
Left inferior frontal gyrus	-50	8	18	1.97	14
Left thalamus	-16	-28	6	2.07	11
Right putamen	18	12	0	1.81	5
Right > Left GPi					
Right globus pallidus	16	-4	-10	8.12	564
Left insula	-34	10	-6	3.94	343
Right inferior parietal lobule	54	18	20	3.12	136
Right inferior frontal gyrus	38	30	-4	2.89	126
Right brainstem	4	-28	-2	2.54	103
Right middle cingulate gyrus	12	18	36	2.42	69
Left thalamus	-16	-14	20	3.26	57
Right inferior frontal gyrus	60	12	6	2.53	56
Left subcallosal gyrus	-18	4	-16	2.62	29
Right rolandic operculum	50	4	4	2.09	13
Right supplementary motor area	12	2	68	2.23	8
Left putamen	-28	-2	-6	2.39	7

Peak MNI coordinates, z-scores, and volumes are reported for clusters demonstrating significant differences between ALE maps derived from left and right hemisphere seeds of STN and GPi ($P > 0.95$).

The insula was found to have greater coactivation with STN than GPi. In the functional parcellation scheme of STN proposed by Lambert et al. [2012], projections from STN to the posterior insula constitute a portion of the STN motor network. However, the sensorimotor area of the insula extends beyond the posterior aspect to the middle region of the insula [Kurth et al., 2010]. In this study, greater STN coactivation was indeed found in the middle insula, likely reflecting the cortico-subcortical connections in the STN motor network.

Connectivity of STN and GPi to Speech Regions

The second aim of this study was to examine the convergence of STN and GPi MACMs with an activation map representing the functional speech network. Our conjunction of

Speech and STN resulted in subcortical activations in left VLN, putamen, GPi, and right red nucleus. The analysis further resulted in significant cortical activation in the left insula. Meanwhile, our conjunction of Speech and GPi revealed subcortical connections with the left VLN, putamen, and right thalamus. However, this conjunction also revealed a significant intersection of coactivation maps in both the left insula and SMA.

To supplement the conjunction of Speech \cap STN and Speech \cap GPi, we also performed conjunction analyses between the Speech ALE maps and the statistical contrasts from each of the ROIs (STN > GPi and GPi > STN) to assess whether the differences in coactivation between STN and GPi would present in areas of the speech network. Regions emerging from the STN > GPi contrast intersected with four regions found to be active in a meta-analysis of speech-related tasks—the left putamen, left

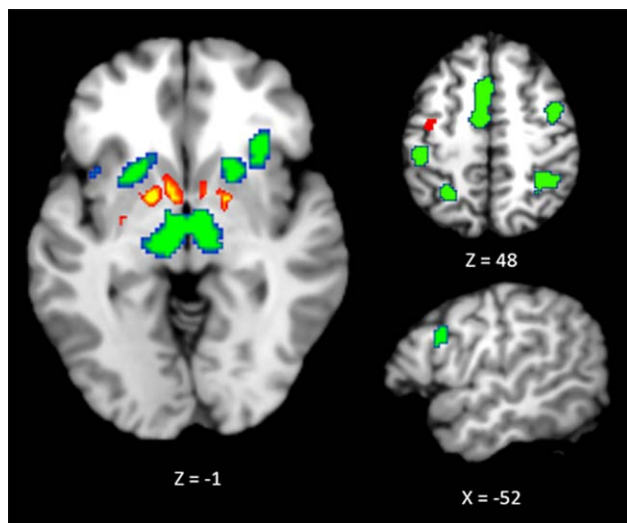


Figure 2.

Contrast of STN and GPi connectivity maps. Blue-green regions correspond to the contrast of STN > GPi ($P > 0.95$). Red-yellow regions correspond to the contrast of GPi > STN ($P > 0.95$).

dorsal anterior insula, left pre-SMA, and left inferior frontal gyrus (BA 44). Meanwhile the GPi > STN contrast intersected with the speech network in the left ventral anterior insula, left dorsal SMA, left premotor cortex, and left middle insula.

Left insula

In this study, significant coactivation with the left insula was observed for both STN and GPi seeds in conjunction with speech network. The left insula is one of several regions included in the “minimal brain network” of speech motor control [Ackermann and Reicker, 2010; Guenther, 2006]. In particular, the anterior portion of the left insula has been linked to overt speech production [Ackermann and Reicker, 2004; Brown et al., 2005], articulatory planning [Dronkers, 1996; Wise et al., 1999], segmental processing [Ackerman and Reicker, 2004], and compensating for perturbations in voice F0 [Zarate et al., 2010]. Decrements in insular rCBF have been observed in patients with PD [Kikuchi et al., 2001]. In addition, these decrements have been shown to correlate with PD disease progression and may be related to PD symptoms that are DOPA-refractory [Kikuchi et al., 2001]. If thalamocortical connections to the insula are in fact unresponsive to dopaminergic medication, it could explain why certain speech functions are unresponsive to pharmacological treatment.

Contrasts of STN and GPi connectivity maps also revealed differential connectivity to the insula. Specifically, the intersection of STN > GPi with Speech resulted in connections to a dorsal anterior portion of the insula while the intersection of GPi > STN with Speech resulted in con-

nections to a more ventral area ranging from middle to anterior insula. Other studies have described similar regions following a functional parcellation of the insula [Chang et al., 2013; Kurth et al., 2010]. The dorsal anterior portion of the insula has been found to be involved in cognitive processes [Chang et al., 2013; Kurth et al., 2010], speech [Kurth et al., 2010], and focal attention [Nelson et al., 2010]. By contrast, studies have shown the ventral anterior insula to be involved in emotional processes, while the middle (central) insula appears to be involved in sensorimotor function [Kurth et al., 2010]. One explanation for the differences observed in the present meta-analysis is that the roles of STN and GPi connections to speech regions differ based on their contributions to motor, emotion, and cognitive function. It is possible that functional connections from STN to insula are more involved in cognitive processes while connections from GPi to insula are more involved in motor and emotional components of speech.

Supplementary motor area

SMA is involved in planning and initiation of both overt [Brendel et al., 2010] and covert speech [Ryding et al., 1996]. While it emerges in both STN and GPi connectivity maps, the intersection of MACMs with the speech network only reveal SMA overlap with the MACM of GPi. The intersection of the speech ALE map with the contrast of GPi > STN also revealed activation in SMA proper. Conversely, the conjunction of speech and STN > GPi resulted in a cluster of activation in the ventral pre-SMA, just above the cingulate cortex (Fig. 4). While SMA proper is associated with initiating motor output, pre-SMA is involved in motor planning [Halsband et al., 1993; Shima et al., 1996] and cognition [Forstmann et al., 2008; Zentgraf et al., 2005]. As mentioned previously, a hyperdirect pathway connecting STN to pre-SMA and IFG has been linked to response inhibition [Aron and Poldrack, 2006; Aron et al., 2007]. Relative to speech, pre-SMA appears to be involved in cognitive linguistic components of word production, including word selection and phonological planning [Alario et al., 2006; Zentgraf et al., 2005] while SMA proper is directly involved with the motor processes in overt speech [Peeva et al., 2010]. For instance, it has been proposed that connections between SMA and GPi comprise a BG-thalamocortical loop involved in initiating motor programs at the phonemic level [Peeva et al., 2010]. As the differences in connectivity between our two ROIs show preferential connectivity of STN for pre-SMA and GPi for SMA proper, it is possible that changes in STN function may have a greater impact on linguistic tasks such as phonological planning while GPi may have a greater influence on the initiation and execution of motor speech commands. Given the coactivation of STN with both IFG and pre-SMA, it is also possible that these differences are related to the role of STN in response inhibition [Aron et al., 2007; Duann et al., 2009; Jahfari et al., 2011].

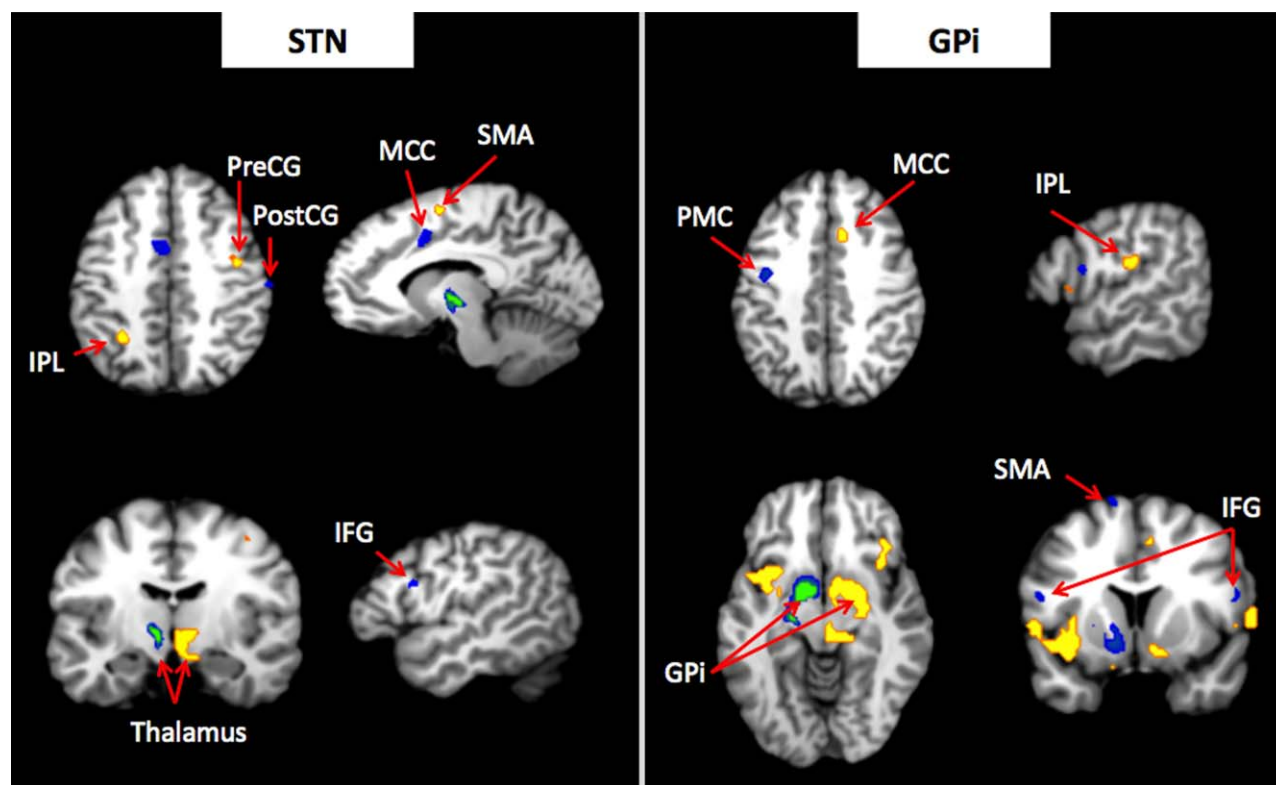


Figure 3.

Contrast of connectivity maps generated from left and right hemisphere seeds. Regions shown in blue-green correspond to Left > Right contrasts ($P > 0.95$) for STN (left) and GPi (right). Regions shown in red-yellow correspond to Right > Left contrasts ($P > 0.95$). Abbreviations: PreCG = precentral gyrus; Post-

CG = postcentral gyrus; IPL = inferior parietal lobule, MCC = middle cingulate cortex; SMA = supplementary motor area; PMC = premotor cortex; IFG = inferior frontal gyrus; GPi = globus pallidus pars interna.

Ventrolateral nucleus

In addition to the left insula, both STN and GPi coactivated with the VLN of the thalamus. The VLN serves as the major relay point for cortico-basal ganglia motor connections [Strick, 1976], receiving direct inhibitory inputs from GPi and indirect inhibitory modulation from STN [Alexander and Crutcher, 1990]. Lesions of the VLN used to treat PD have resulted in speech deficits ranging from mild to severe [Samra et al., 1969]. In addition, stimulation of the VLN has been shown to lead to severe speech disturbances including speech arrest, dysarthria, involuntary vocalization [Petrovici, 1980], and anomia [Ojemann and Ward, 1971]. As expected, both STN and GPi seeds coactivated with the VLN. For STN, however, this coactivation cluster also expanded to include the medial dorsal nucleus. Functional projections from both STN and GPi to the cortical speech network likely involve relay through the VLN, however the MDN may serve as an additional relay for projections from STN.

Inferior frontal gyrus

We observed the emergence of a cluster in left BA 44 from the conjunction of Speech \cap STN > GPi. Like pre-SMA, IFG is involved in both cognitive linguistic processes and response inhibition. Activation in left BA 44 has been linked to phonological verbal fluency [Heim et al., 2009], top-down speech comprehension [Zekveld et al., 2006], and syntactic processing [Friederici, 2002; Kang et al., 1999]. As mentioned above, IFG is also involved in stop-action response inhibition via connections to STN and pre-SMA [Aron et al., 2007]. Patients undergoing STN-DBS report more frequent cognitive disruptions than those undergoing GPi-DBS, most notably in the performance of verbal fluency tasks [Dietz et al., 2013; Parsons et al., 2006]. Schroeder et al. [2003] found that while IFG/insula was active during a word generation task with DBS off, it underwent significant decreases in regional cerebral blood flow (rCBF) when stimulation was turned on. Based on the evidence from previous PET studies as well as data gathered in the

TABLE VI. Regions of the speech ALE map sharing activation with MACMs (Speech \cap STN, Speech \cap GPi) and their respective contrasts (Speech \cap STN > GPi, Speech \cap GPi > STN)

Location	MNI coordinates			z-Score	Size (voxels)
	x	y	z		
Speech \cap STN					
Left thalamus (VLN)	-6	-8	2	2.04	991
Left putamen	-20	8	0	1.76	240
Left insula	-32	18	2	1.31	50
Left GPi	-16	-4	-2	1.15	10
Right red nucleus	6	-22	-4	1.49	9
Speech \cap GPi					
Left putamen	-20	8	-2	2.49	1,707
Left insula	-32	14	-4	2.09	1,111
Left thalamus (VLN)	-6	-8	2	2.16	816
Right thalamus (MDN)	4	-24	-2	2.75	343
Right SMA	8	-4	60	2.51	69
Speech \cap STN > GPi					
Left putamen (mid-post)	-20	6	4	2.01	1,137
Left dorsal anterior insula	-34	22	2	2.01	925
Left pre-SMA	-4	16	44	2.06	601
Left inferior frontal gyrus (BA 44)	-52	16	6	2.45	192
Speech \cap GPi > STN					
Left ventral anterior insula	-32	18	0	2.83	799
Left dorsal SMA	-4	8	62	2.98	121
Left premotor cortex	-52	0	46	2.84	106
Left middle insula	-44	10	0	2.65	73

Peak MNI coordinates, z-scores, and volumes are reported for clusters demonstrating significant intersection of thresholded MACMs and contrasts with the speech ALE map ($P < 0.05$).

Author Queries

present meta-analysis, it is possible that changes in STN function can disrupt verbal fluency or response inhibition by affecting functional connections to left IFG.

Premotor cortex

By contrast, GPi appears to preferentially coactivate with regions that are primarily motor-oriented. In addition to SMA and middle insula, the conjunction of Speech \cap GPi > STN resulted in activation of premotor cortex. When compared to the spatial representations of articulators described by Bouchard et al. [2013], this activation cluster maps closely to the cortical representation of the larynx during speech production. Stimulation of GPi has similarly resulted in increased bloodflow metabolism in premotor cortex in patients with PD [Fukuda et al., 2001]. With respect to speech, premotor cortex is involved in the planning and sequencing of the motor units required for speech production [Halsband et al., 1993] as well as speech perception [Meister et al., 2007]. Given the preferential activation of GPi to premotor cortex, it may be the case that changes in GPi activity are more likely than STN to affect changes in motor planning/sequencing in both speech and general motor control.

Functional Profiles of STN and GPi

We anticipated that the functional profiles of STN and GPi would reflect the known functional diversity of these regions [Temel et al., 2005]. Both regions displayed significant relationships with the action domain, with GPi linked to action inhibition and STN linked to action execution. Behavioral domain analyses also revealed a significant relationship of GPi activation with cognition, emotion, and sexual interoception, corroborating the known roles of GPi in motor, associative, and limbic cortico-basal ganglia circuits. By contrast, the only additional behavioral domain linked to STN activation was pain perception. That speech domains did not emerge from the functional characterization analysis of either seed is not surprising given that both regions likely play an indirect role in speech function via thalamocortical connections. Though STN and GPi may not be active during speech tasks, both regions are functionally connected with cortical and subcortical areas that support speech function.

Limitations and Future Directions

There are a few limitations of this study to consider. As mentioned previously, the two ROIs used, while

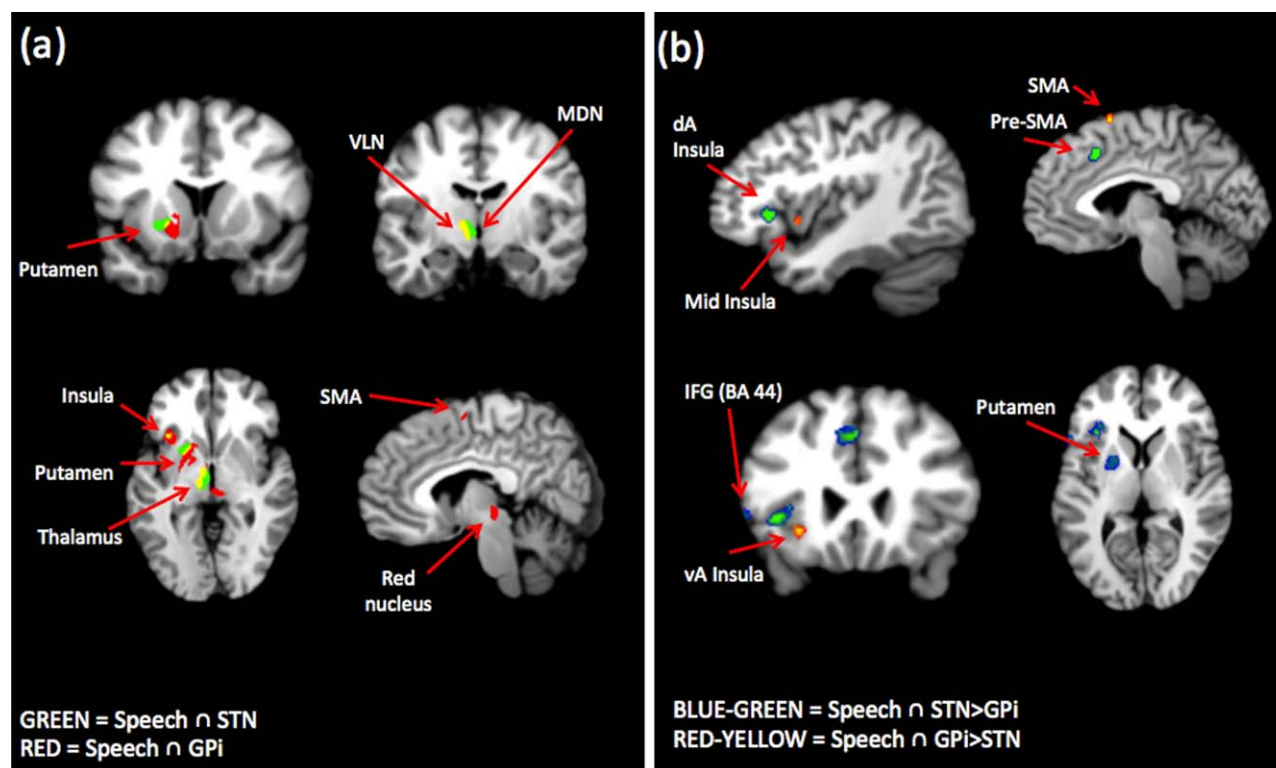


Figure 4.

(a) Conjunction of STN and GPI MACMs to speech meta-analysis. Blue-green clusters correspond to Speech ∩ STN. Red-yellow clusters correspond to Speech ∩ GPI. (b) Conjunction of STN > GPI and GPI > STN contrasts to speech meta-analysis. Blue-green clusters correspond to Speech ∩ STN > GPI. Red-

yellow clusters correspond to Speech ∩ GPI > STN. Abbreviations: SMA = supplementary motor area; VLN = ventral lateral nucleus; MDN = medial dorsal nucleus; dA Insula = dorsal anterior insula; vA Insula = ventral anterior insula; IFG = inferior frontal gyrus.

anatomically defined, were very different in size (STN = 254 mm³, GPI = 1,138 mm³). Yet despite an approximate 4.5:1 difference in volume, our search of the Brain-Map database yielded only twice as many experiments reporting coactivations with GPI than it did for STN. As the method used for computing statistical contrasts of ALE maps accounts for differences in the number of experiments gathered for each ROI, it is unlikely that the results of our contrast analyses were impacted by differences in ROI volume. Additionally, this study did not include experiments reporting de-activations. As many PET studies reported decreases in rCBF following STN DBS, it is possible that we did not include regions whose activity is inversely related to that of our ROIs.

Importantly, while the meta-analytic connectivity of STN and GPI may serve as a guide for generating hypotheses about the roles of STN and GPI in speech function, deriving the relationship of individual BG-thalamocortical connections in specific speech processes would require a more tailored approach. For example, future studies could investigate the effective connectivity of GPI-thalamocortical

loops during phonation or syllable repetition. Likewise, one could examine the modulation of STN-cortical connections during the performance of a verbal fluency task. Studies examining functional connectivity of STN and GPI during the performance of speech tasks would further allow us to understand the involvement of these areas in specific speech functions (e.g., verbal fluency versus motor sequencing). As this analysis focused on healthy subjects, similar connectivity analyses in patient populations would also be necessary to determine if these findings can be expanded to explain speech changes associated with BG dysfunction.

CONCLUSIONS

The connectivity models of our STN and GPI seeds showed expected coactivation with the thalamus and other basal ganglia nuclei (putamen, caudate, STN, and pallidum). In addition to subcortical structures, both seed regions shared coactivations with SMA, IFG, and insula;

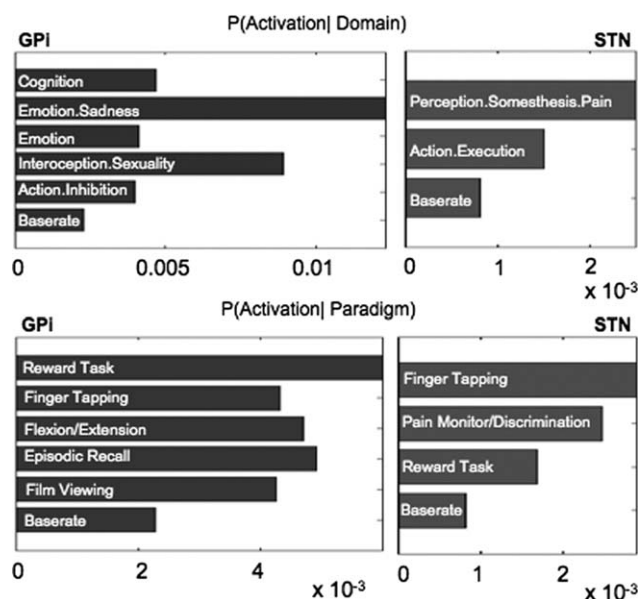


Figure 5.

Results of the functional characterization analyses for STN and GPi. Red bars indicate the probability of observing activation within GPi when constrained by behavioral domain (above) and by paradigm class (below). Green bars indicate the probability of observing activation within STN when constrained by behavioral domain (above) and paradigm class (below). All results depicted were thresholded at $P < 0.01$, uncorrected.

however, there were also significant coactivation differences within these regions. For instance, SMA and insula were more likely to coactivate with STN than GPi. Additionally, premotor cortex was more likely to coactivate with GPi than STN. The shared functional connections of STN and GPi likely emerge from shared cortico-basal ganglia pathways (e.g., the indirect pathway from BG to SMA). By contrast, coactivation differences may reflect the presence of additional functional connections beyond the indirect pathway (e.g., the additional connectivity of STN to SMA via a hyperdirect pathway).

Meta-analytic connectivity maps also depict functional connections of both STN and GPi to regions within the speech network. This study revealed a tendency for STN to have stronger connectivity than GPi with regions involved in cognitive linguistic processing and response inhibition (pre-SMA, dorsal anterior insula, and IFG), while GPi demonstrated stronger connectivity than STN to regions involved in motor-oriented speech function (middle insula, SMA, and premotor cortex).

REFERENCES

Ackermann H, Riecker A (2004): The contribution of the insula to motor aspects of speech production: A review and a hypothesis. *Brain Lang* 89:320–328.

Ackermann H, Riecker A (2010): The contribution (s) of the insula to speech production: A review of the clinical and functional imaging literature. *Brain Struct Funct* 214:419–433.

Alario F, Chainay H, Lehericy S, Cohen L (2006): The role of the supplementary motor area (SMA) in word production. *Brain Res* 1076:129–143.

Alexander GE, DeLong MR, Strick PL (1986): Parallel organization of functionally segregated circuits linking basal ganglia and cortex. *Annu Rev Neurosci* 9:357–381.

Alexander GE, Crutcher MD (1990): Functional architecture of basal ganglia circuits: Neural substrates of parallel processing. *Trends Neurosci* 13:266–271.

Alexander GE (1994): Basal ganglia-thalamocortical circuits: Their role in control of movements. *J Clin Neurophysiol* 11:420–431.

Alm PA (2004): Stuttering and the basal ganglia circuits: A critical review of possible relations. *J Commun Disord* 37:325–369.

Ali SO, Thomassen M, Schulz GM, Hosey LA, Varga M, Ludlow CL, Braun AR (2006): Alterations in CNS activity induced by botulinum toxin treatment in spasmodic dysphonia: An H215O PET study. *J Speech Lang Hear Res* 49:1127.

Aron AR, Poldrack RA (2006): Cortical and subcortical contributions to stop signal response inhibition: Role of the subthalamic nucleus. *J Neurosci* 26:2424–2433.

Aron AR, Behrens TE, Smith S, Frank MJ, Poldrack RA (2007): Triangulating a cognitive control network using diffusion-weighted magnetic resonance imaging (MRI) and functional MRI. *J Neurosci* 27:3743–3752.

Ballanger B, Jahanshahi M, Broussolle E, Thobois S (2009): PET functional imaging of deep brain stimulation in movement disorders and psychiatry. *J Cereb Blood Flow Metab* 29:1743–1754.

Baudrexel S, Witte T, Seifried C, Von Wegner F, Beissner F, Klein JC, Steinmetz H., Deichmann R, Roeper J, Hilker R (2011): Resting state fMRI reveals increased subthalamic nucleus–motor cortex connectivity in Parkinson’s disease. *Neuroimage* 55:1728–1738.

Bouchard KE, Mesgarani N, Johnson K, Chang EF (2013): Functional organization of human sensorimotor cortex for speech articulation. *Nature* 495:327–332.

Brendel B, Hertrich I, Erb M, Lindner A, Riecker A, Grodd W, Ackermann H (2010): The contribution of mesiofrontal cortex to the preparation and execution of repetitive syllable productions: An fMRI study. *Neuroimage* 50:1219–1230.

Brown S, Ingham RJ, Ingham JC, Laird AR, Fox PT (2005): Stuttered and fluent speech production: An ALE meta-analysis of functional neuroimaging studies. *Hum Brain Mapp* 25:105–117.

Brunenberg EJJ, Moeskops P, Backes WH, Pollo C, Cammoun L, Vilanova A, Janssen MLF, Visser-Vanderwalle VERM, ter Haar Romeny BM, Thiran J, Platel B (2012): Structural and resting state functional connectivity of the subthalamic nucleus: Identification of motor STN parts and the hyperdirect pathway. *PLoS One* 7:e39061.

Cauda F, Costa T, Torta DM, Sacco K, D’Agata F, Duca S, Geminiani G, Fox PT, Vercelli A (2012): Meta-analytic clustering of the insular cortex: Characterizing the meta-analytic connectivity of the insula when involved in active tasks. *Neuroimage* 62:343–355.

Civier O, Bullock D, Max L, Guenther FH (2013): Computational modeling of stuttering caused by impairments in a basal ganglia thalamo-cortical circuit involved in syllable selection and initiation. *Brain Lang* 126:263–278.

- Chang LJ, Yarkoni T, Khaw MW, Sanfey AG (2013): Decoding the role of the insula in human cognition: Functional parcellation and large-scale reverse inference. *Cereb Cortex* 23:739–749.
- Dietz J, Noecker AM, McIntyre CC, Bowers D, Foote KD, Okun MS (2013): Stimulation region within the globus pallidus does not affect verbal fluency performance. *Brain Stimul* 6:248–253.
- Di Martino A, Scheres A, Margulies DS, Kelly AMC, Uddin LQ, Shehzad Z, Biswal B, Walters JR, Castellanos FX, Milham MP (2008): Functional connectivity of human striatum: A resting state fMRI study. *Cereb Cortex* 18:2735–2747.
- Draganski B, Kherif F Klöppel S, Cook PA, Alexander DC, Parker GJ, Deichmann R, Ashburner J, Frackowiak RS (2008): Evidence for segregated and integrative connectivity patterns in the human basal ganglia. *The Journal of Neuroscience* 28: 7143–7152.
- Dromey C, Bjarnason S (2011): A preliminary report on disordered speech with deep brain stimulation in individuals with Parkinson's disease. *Parkinsons Dis* 2011:796205.
- Dronkers NF (1996): A new brain region for coordinating speech articulation. *Nature* 384:159–161.
- Duann JR, Ide JS, Luo X, Li CSR (2009): Functional connectivity delineates distinct roles of the inferior frontal cortex and pre-supplementary motor area in stop signal inhibition. *J Neurosci* 29:10171–10179.
- Dubois B, Pillon B (1996): Cognitive deficits in Parkinson's disease. *J Neurol* 244:2–8.
- Duffy JR (2012): *Motor Speech Disorders: Substrates, Differential Diagnosis, and Management*. St. Louis, MO: Mosby Incorporated.
- Eccles JC (1982): The initiation of voluntary movements by the supplementary motor area. *Arch Psychiatr Nervenkr* 231:423–441.
- Eickhoff SB, Laird AR, Grefkes C, Wang LE, Zilles K, Fox PT (2009): Coordinate-based activation likelihood estimation meta-analysis of neuroimaging data: A random-effects approach based on empirical estimates of spatial uncertainty. *Hum Brain Mapp* 30:2907–2926.
- Eickhoff SB, Bzdok D, Laird AR, Roski C, Caspers S, Zilles K, Fox PT (2011): Co-activation patterns distinguish cortical modules, their connectivity and functional differentiation. *Neuroimage* 57:938–949.
- Eickhoff SB, Bzdok D, Laird AR, Kurth F, Fox PT (2012): Activation likelihood estimation meta-analysis revisited. *Neuroimage* 59:2349–2361.
- Farina E, Cappa SF, Polimeni M, Magni E, Canesi M, Zecchinelli A, Scarlato G, Mariani C (1994): Frontal dysfunction in early Parkinson's diseases. *Acta Neurol Scand* 90:34–38.
- Forstmann BU, Dutilh G, Brown S, Neumann J, von Cramon DY, Ridderinkhof KR, Wagenmakers EJ (2008): Striatum and pre-SMA facilitate decision-making under time pressure. *Proc Natl Acad Sci USA* 105:17538–17542.
- Fox PT, Ingham RJ, Ingham JC, Hirsch TB, Downs JH, Martin C, Jerabek P, Glass T, Lancaster JL (1996): A PET study of the neural systems of stuttering. *Nature* 382:158–162.
- Friederici AD (2002): Towards a neural basis of auditory sentence processing. *Trends Cogn Sci* 6:78–84.
- Fukuda M, Mentis M, Ghilardi MF, Dhawan V, Antonini A, Hammerstad J, Lozano AM, Lang A, Lyons K, Ghez C, Eidelberg D (2001): Functional correlates of pallidal stimulation for Parkinson's disease. *Ann Neurol* 49:155–164.
- Gerardin E, Sirigu A, Lehericy S, Poline JB, Gaymard B, Marsault C, Agid Y, Le Bihan D (2000): Partially overlapping neural networks for real and imagined hand movements. *Cereb Cortex* 10:1093–1104.
- Grafton ST, Arbib MA, Fadiga L, Rizzolatti G (1996): Localization of grasp representations in humans by positron emission tomography. *Exp Brain Res* 112:103–111.
- Guenther FH (2006): Cortical interactions underlying the production of speech sounds. *J Commun Disord* 39:350–365.
- Halsband U, Ito N, Tanji J, Freund HJ (1993): The role of premotor cortex and the supplementary motor area in the temporal control of movement in man. *Brain* 116:243–266.
- Hanakawa T, Dimyan MA, Hallett M (2008): Motor planning, imagery, and execution in the distributed motor network: A time-course study with functional MRI. *Cereb Cortex* 18:2775–2788.
- Haslinger B, Erhard P, Dresel C, Castrop F, Roettinger M, Ceballos-Baumann AO (2005): "Silent event-related" fMRI reveals reduced sensorimotor activation in laryngeal dystonia. *Neurology* 65:1562–1569.
- Hazarati LN, Parent A (1992): Convergence of subthalamic and striatal efferents at pallidal level in primates: An anterograde double-labeling study with biocytin and PHA-L. *Brain Res* 569: 336–340.
- Heim S, Eickhoff SB, Amunts K (2009): Different roles of cytoarchitectonic BA 44 and BA 45 in phonological and semantic verbal fluency as revealed by dynamic causal modelling. *Neuroimage* 48:616–624.
- Hershey T, Black KJ, Carl JL, McGee-Minnich L, Snyder AZ, Perlmuter JS (2003): Long term treatment and disease severity change brain responses to levodopa in Parkinson's disease. *J Neurol Neurosurg Psychiatry* 74:844–851.
- Jacobs DH, Shuren J, Bowers D, Heilman KM (1995): Emotional facial imagery, perception, and expression in Parkinson's disease. *Neurology* 45:1696–1702.
- Jahfari S, Waldorp L, van den Wildenberg WP, Scholte HS, Ridderinkhof KR, Forstmann BU (2011): Effective connectivity reveals important roles for both the hyperdirect (fronto-subthalamic) and the indirect (fronto-striatal-pallidal) fronto-basal ganglia pathways during response inhibition. *J Neurosci* 31: 6891–6899.
- Joel D, Weiner I (1994): The organization of the basal ganglia-thalamocortical circuits: Open interconnected rather than closed segregated. *Neuroscience* 63:363–379.
- Joel D (2001): Open interconnected model of basal ganglia-thalamocortical circuitry and its relevance to the clinical syndrome of Huntington's disease. *Movement Disord* 16:407–423.
- Kang AM, Constable RT, Gore JC, Avrutin S (1999): An event-related fMRI study of implicit phrase-level syntactic and semantic processing. *Neuroimage* 10:555–561.
- Karimi M, Golchin N, Tabbal SD, Hershey T, Videen TO, Wu J, Usche JW, Revilla FJ, Hartlein JM, Wenie AR, Mink JW, Perlmuter JS (2008): Subthalamic nucleus stimulation-induced regional blood flow responses correlate with improvement of motor signs in Parkinson disease. *Brain* 131:2710–2719.
- Kikuchi A, Takeda A, Kimpara T, Nakagawa M, Kawashima R, Sugiura M, Kinomura S, Fukuda H, Chida K, Okita N, Takase S, Itoyama Y (2001): Hypoperfusion in the supplementary motor area, dorsolateral prefrontal cortex and insular cortex in Parkinson's disease. *J Neurol Sci* 193:29–36.
- Klostermann F, Ehlen F, Vesper J, Nubel K, Gross M, Marzinzik F, Curio G, Sappok T (2008): Effects of subthalamic deep brain stimulation on dysarthrophonia in Parkinson's disease. *J Neurol Neurosurg Psychiatry* 79:522–529.

- Kurth F, Zilles K, Fox PT, Laird AR, Eickhoff SB (2010): A link between the systems: functional differentiation and integration within the human insula revealed by meta-analysis. *Brain Struct Funct* 214:519–534.
- Laird AR, Eickhoff SB, Li K, Robin DA, Glahn DC, Fox PT (2009): Investigating the functional heterogeneity of the default mode network using coordinate-based meta-analytic modeling. *J Neurosci* 29:14496–14505.
- Laird AR, Fox PM, Eickhoff SB, Turner JA, Ray KL, McKay DR, Glahn DC, Beckmann CF, Smith SM, Fox PT (2011): Behavioral interpretations of intrinsic connectivity networks. *J Cognitive Neurosci* 23:4022–4037.
- Lambert C, Zrinzo L, Nagy Z, Lutti A, Hariz M, Foltynie T, Draganski B, Ashburner J, Frackowiak R (2012): Confirmation of functional zones within the human subthalamic nucleus: Patterns of connectivity and sub-parcellation using diffusion weighted imaging. *Neuroimage* 60:83–94.
- Liotti M, Ramig LO, Vogel D, New P, Cook CI, Ingham RJ, Ingham JC, Fox PT (2003): Hypophonia in Parkinson's disease neural correlates of voice treatment revealed by PET. *Neurology* 60:432–440.
- Meister IG, Wilson SM, Deblieck C, Wu AD, Iacoboni M (2007): The essential role of premotor cortex in speech perception. *Curr Biol* 17:1692–1696.
- Middleton FA, Strick PL (2000): Basal ganglia and cerebellar loops: Motor and cognitive circuits. *Brain Res Rev* 31:236–250.
- Murdoch BE (2010): Surgical approaches to treatment of Parkinson's disease: Implications for speech function. *Int J Speech Lang Pathol* 12:375–384.
- Narayana S, Jacks A, Robin DA, Poizner H, Zhang W, Franklin C, Liotti M, Vogel D, Fox PT (2009): A noninvasive imaging approach to understanding speech changes following deep brain stimulation in Parkinson's disease. *Am J Speech Lang Pathol* 18:146–161.
- Nelson SM, Dosenbach NU, Cohen AL, Wheeler ME, Schlaggar BL, Petersen SE (2010): Role of the anterior insula in task-level control and focal attention. *Brain Struct Funct* 214:669–680.
- Obeso JA, Marin C, Rodriguez-Oroz C, Blesa J, Benitez-Temiño B, Mena-Segovia J, Rodríguez M, Olanow CW (2008): The basal ganglia in Parkinson's disease: current concepts and unexplained observations. *Annals of neurology* 64:S30–S46.
- Ojemann GA, Ward AA (1971): Speech representation in ventrolateral thalamus. *Brain* 94:669–680.
- Parent A (1990): Extrinsic connections of the basal ganglia. *Trends in neurosciences* 13:254–258.
- Parent A, Hazarati LN (1995): Functional anatomy of the basal ganglia. II. The place of subthalamic nucleus and external pallidum in basal ganglia circuitry. *Brain Res Rev* 20:128–154.
- Parsons TD, Rogers SA, Braaten AJ, Woods SP, Tröster AI (2006): Cognitive sequelae of subthalamic nucleus deep brain stimulation in Parkinson's disease: A meta-analysis. *Lancet Neurol* 5: 578–588.
- Peeva MG, Guenther FH, Tourville JA, Nieto-Castanon A, Anton JL, Nazarian B, Alario FX (2010): Distinct representations of phonemes, syllables, and supra-syllabic sequences in the speech production network. *Neuroimage* 50:626–638.
- Petrovici JN (1980): Speech disturbances following stereotaxic surgery in ventrolateral thalamus. *Neurosurg Rev* 3:189–195.
- Postuma RB, Dagher A (2006): Basal ganglia functional connectivity based on a meta-analysis of 126 positron emission tomography and functional magnetic resonance imaging publications. *Cereb cortex* 16:1508–1521.
- Robinson JL, Laird AR, Glahn DC, Lovallo WR, Fox PT (2010): Metaanalytic connectivity modeling: Delineating the functional connectivity of the human amygdala. *Hum Brain Mapp* 31: 173–184.
- Robinson JL, Laird AR, Glahn DC, Blangero J, Sanghera MK, Pessoa L, Fox PM, Uecker A, Friehs G, Young KA, Griffin JL, Lovallo WR, Fox PT (2012): The functional connectivity of the human caudate: An application of meta-analytic connectivity modeling with behavioral filtering. *NeuroImage* 60:117–129.
- Ryding E, BraÅdvik B, Ingvar DH (1996): Silent speech activates prefrontal cortical regions asymmetrically, as well as speech-related areas in the dominant hemisphere. *Brain Lang* 52:435–451.
- Samra K, Riklan M, Levita E, Zimmerman J, Waltz JM, Bergmann L, Cooper IS (1969): Language and speech correlates of anatomically verified lesions in thalamic surgery for parkinsonism. *J Speech Lang Hear Res* 12:510–540.
- Schroeder U, Kuehler A, Lange KW, Haslinger B, Tronnier VM, Krause M, Pfister R, Boecker H, Caballos-Baumann AO (2003): Subthalamic nucleus stimulation affects a frontotemporal network: A PET study. *Ann Neurol* 54:445–450.
- Scott R, Gregory R, Hines N, Carroll C, Hyman N, Papanastasiou V, Leather C, Rowe J, Silburn P, Aziz T (1998): Neuropsychological and functional outcome following pallidotomy for Parkinson's disease. A consecutive series of eight simultaneous bilateral and twelve unilateral procedures. *Brain* 121:659–675.
- Shima K, Mushiake H, Saito N, Tanji J (1996): Role for cells in the presupplementary motor area in updating motor plans. *Proc Natl Acad Sci USA* 93:8694–8698.
- Simonyan K, Herscovitch P, Horwitz B (2013): Speech-induced striatal dopamine release is left lateralized and coupled to functional striatal circuits in healthy humans: A combined PET, fMRI and DTI study. *Neuroimage* 70:21–32.
- Simonyan K, Ludlow CL (2010): Abnormal activation of the primary somatosensory cortex in spasmodic dysphonia: An fMRI study. *Cerebral Cortex* 20:2749–2759.
- Smith SM, Fox PT, Miller KL, Glahn DC, Fox PM, Mackay CE, Filippini N, Watkins KE, Toro R, Laird AR, Beckmann CF (2009): Correspondence of the brain's functional architecture during activation and rest. *Proc Natl Acad Sci USA* 106:13040–13045.
- Strick PL (1976): Anatomical analysis of ventrolateral thalamic input to primate motor cortex. *J Neurophysiol* 39:1020–1031.
- Tasker RR, Lang AE, Lozano AM (1997): Pallidal and thalamic surgery for Parkinson's disease. *Exp Neurol* 144:35–40.
- Temel Y, Blokland A, Steinbusch HW, Visser-Vandewalle V (2005): The functional role of the subthalamic nucleus in cognitive and limbic circuits. *Prog Neurobiol* 76:393–413.
- Theodoros DG, Ward EC, Murdoch BE, Silburn P, Lethlean J (2000): The impact of pallidotomy on motor speech function in Parkinson disease. *J Med Speech-Lang Path* 8:315–322.
- Thiel A, Hilker R, Kessler J, Habedank B, Herholz K, Heiss WD (2003): Activation of basal ganglia loops in idiopathic Parkinson's disease: A PET study. *J Neural Trans* 110:1289–1301.
- Torta DM, Cauda F (2011): Different functions in the cingulate cortex, a meta-analytic connectivity modeling study. *Neuroimage* 56:2157–2172.
- Turkeltaub PE, Eden GF, Jones KM, Zeffiro TA (2002): Meta-analysis of the functional neuroanatomy of single-word reading: Method and validation. *Neuroimage* 16:765–780.
- Turkeltaub PE, Eickhoff SB, Laird AR, Fox M, Wiener M, Fox P (2012): Minimizing within-experiment and within-group effects

- in activation likelihood estimation meta-analyses. *Hum Brain Mapp* 33:1–13.
- Watkins KE, Smith SM, Davis S, Howell P (2008): Structural and functional abnormalities of the motor system in developmental stuttering. *Brain* 131:50–59.
- Wise RJS, Greene J, Büchel C, Scott SK (1999): Brain regions involved in articulation. *Lancet* 353:1057–1061.
- Wu JC, Maguire G, Riley G, Lee A, Keator D, Tang C, Fallon J, Najafi A (1997): Increased dopamine activity associated with stuttering. *Neuroreport* 8:767–770.
- Zarate JM, Wood S, Zatorre RJ (2010): Neural networks involved in voluntary and involuntary vocal pitch regulation in experienced singers. *Neuropsychologia* 48:607–618.
- Zekveld AA, Heslenfeld DJ, Festen JM, Schoonhoven R (2006): Top-down and bottom-up processes in speech comprehension. *Neuroimage* 32:1826–1836.
- Zentgraf K, Stark R, Reiser M, Künzell S, Schienle A, Kirsch P, Walter B, Vaitl D, Munzert J (2005): Differential activation of pre-SMA and SMA proper during action observation: Effects of instructions. *Neuroimage* 26:662–672.